Electronic Supplementary Material (ESI) for Journal of Materials Chemistry A.

Application of Pyrene-Derived Benzimidizole-Linked Polymers to CO_2 Separation under Pressure and Vacuum Swing Adsorption Settings

Ali Kemal Sekizkardes, Timur İslamoğlu, Zafer Kahveci and Hani M. El-Kaderi*

Department of Chemistry, Virginia Commonwealth University, 1001 W. Main St.,

Richmond, VA 23284-2006, US. Fax: (804) 828-8599; Tel.: (804) 828-7505; E-mail: helkaderi@vcu.edu

Table of Content

Section 1: Characterization of BILPs

Figure S1: TGA traces of BILP-11, BILP-12, BILP-13.

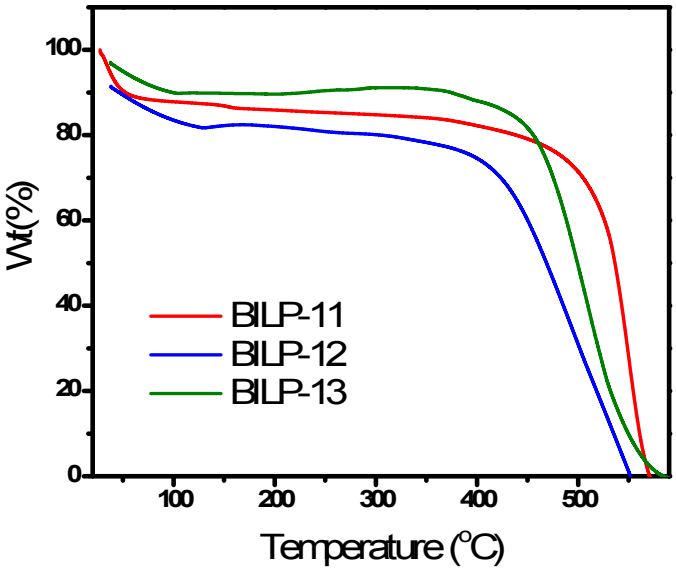

Figure S2: XRD-patterns for BILP-11, BILP-12, BILP-13, indicating the amorphous characteristics of polymers.

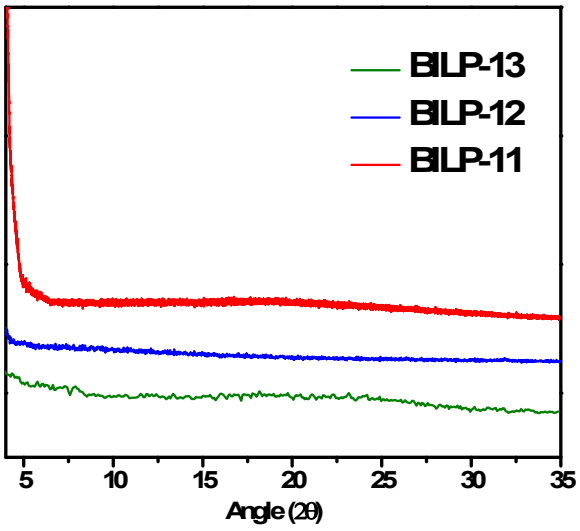

Figure S3: SEM images of BILP-11, BILP-12, BILP-13.

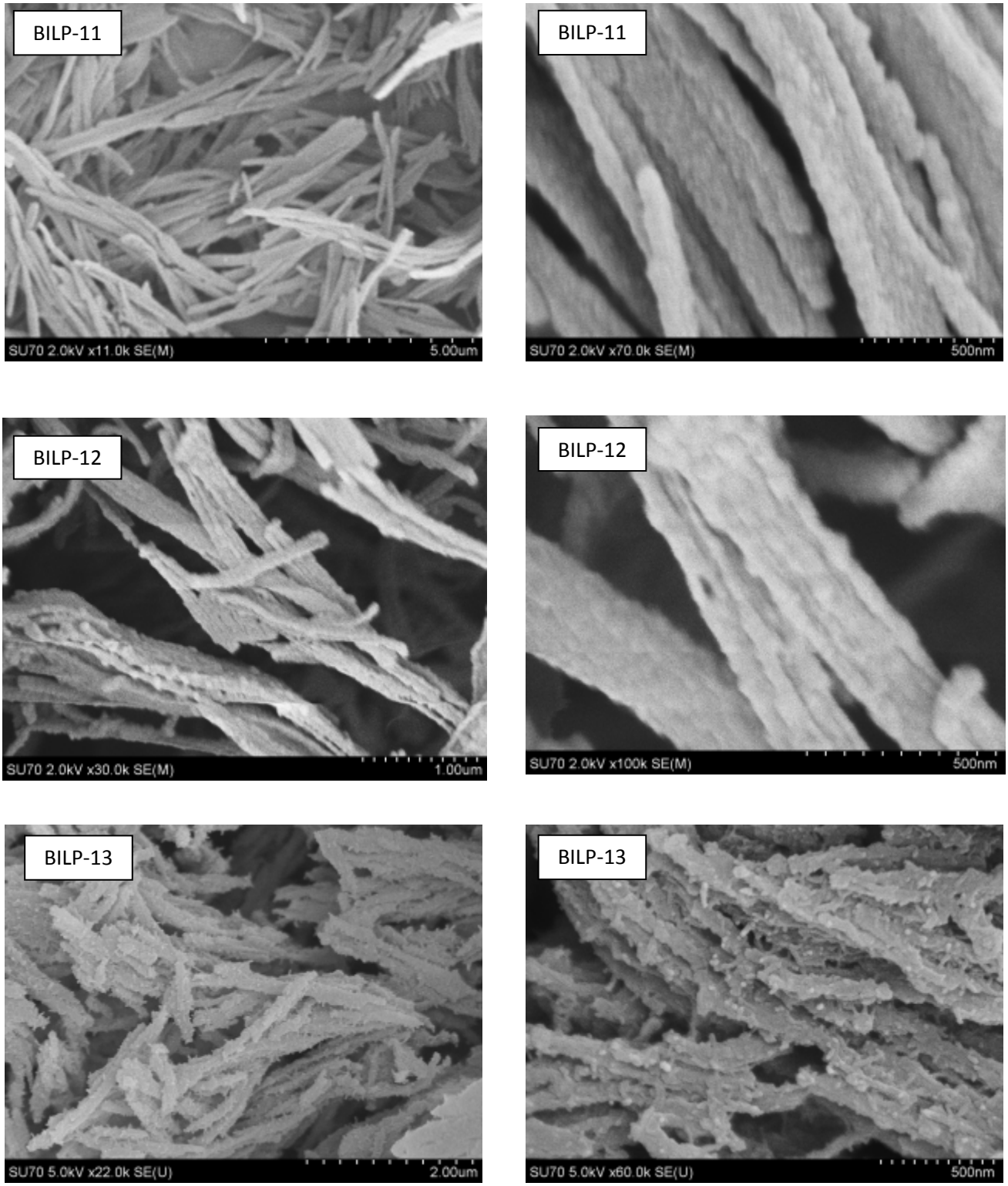

Figure S4: FT-IR spectra of BILP-11, BILP-12, BILP-13 and their starting building units. Lower panel is an expanded region from 500 to 2000 cm^{-1}.

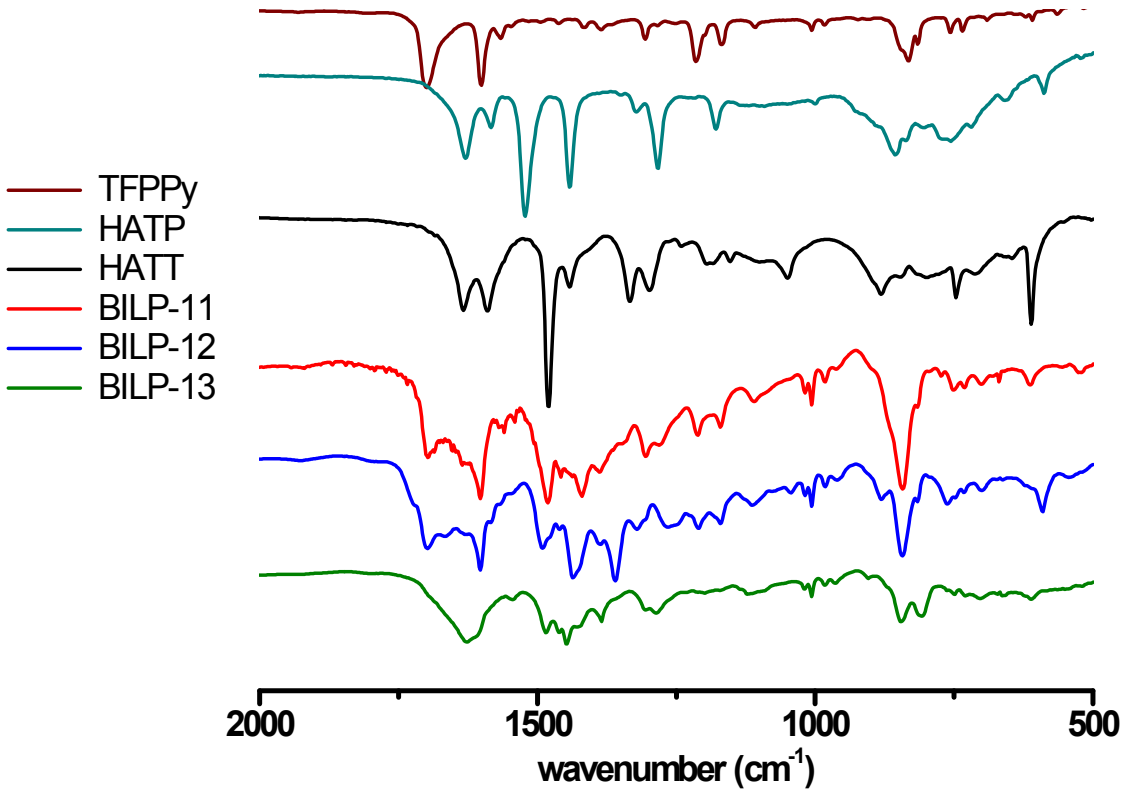

Figure S5: FT-IR spectra (500-4000 cm^{-1}) of starting materials and polymers.

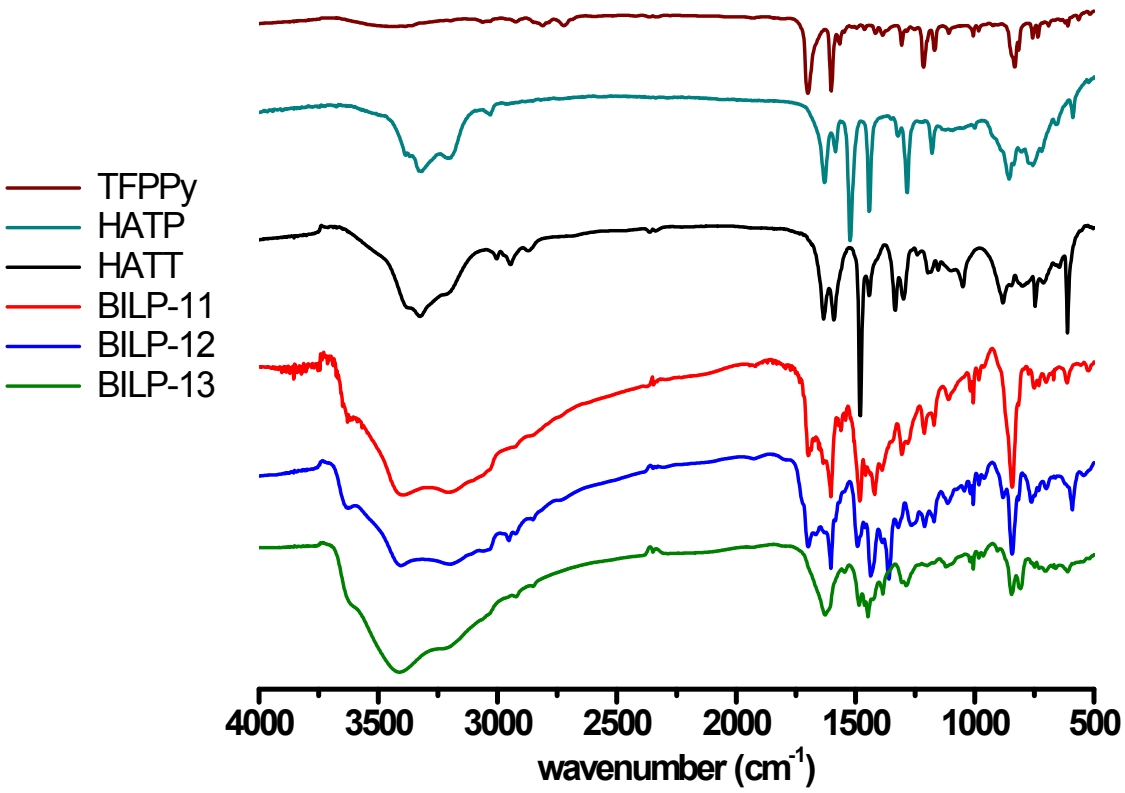

Figure S6: Solid state ^{13}C CP-MAS NMR spectra of BILP-11, BILP-12 and BILP-13.

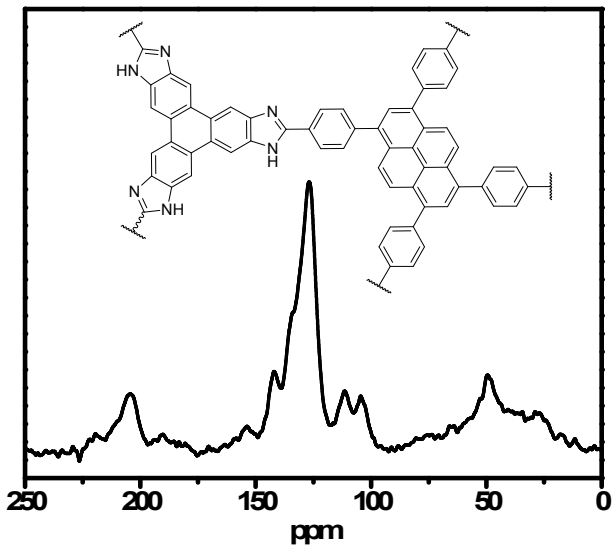

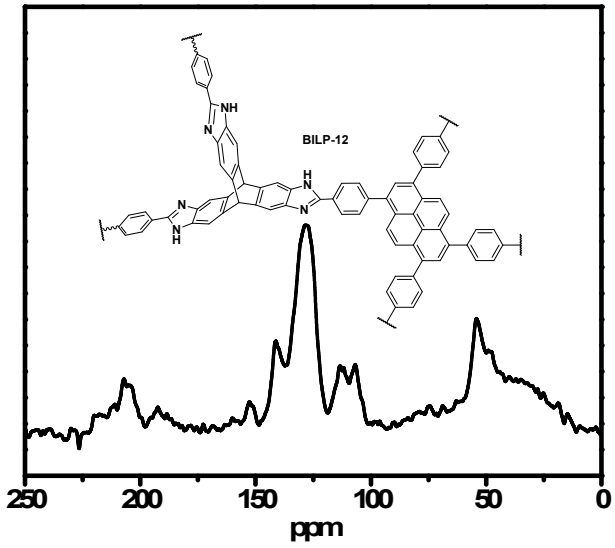

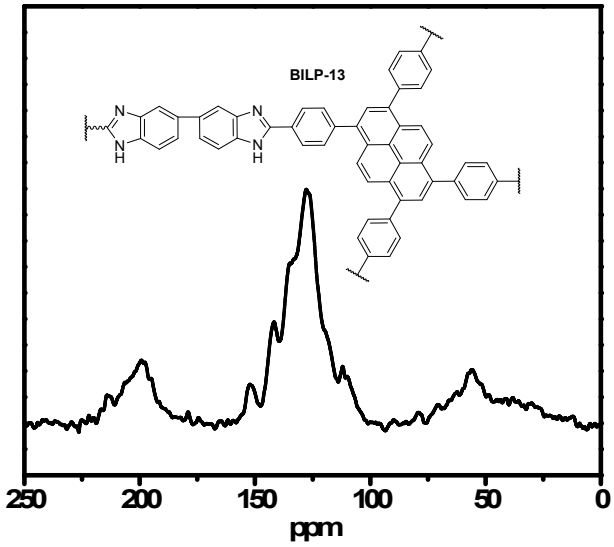

Table S1. Assignments of the ^{13}C CP-MAS NMR peaks for BILPs.

Peaks (ppm)	Peaks (ppm)	Peaks (ppm)	Assignments/Comments
BILP-11	**BILP-12**	**BILP-13**	
	54		Triptycene aliphatic CH.
104			Triphenylene aromatic CH(1) which is observed at 107 ppm in HATP.[1] (d_6-DMSO)
107			Triptycene aromatic CH(2). The peak is observed at 111 ppm in HATT.[2] (d_6-DMSO)
	111		Triphenylene aromatic C(2). The peak is observed at 121 ppm in HATT.[2] (d_6-DMSO)
113			Triptycene aromatic C(3). The peak is observed at 131 ppm in HATT.[2] (d_6-DMSO).
153	152	152	Benzimidizole ring C in C=N. There is no peak was observed at around 160 for imine C=N showing formation of benzimidizole ring.[3]

Section 2: Low-Pressure (0 – 1.0 bar) Gas Adsorption Measurements.

Activation of polymers for gas adsorption measurements: A sample was loaded into a 9 mm large bulb cell (from Quantachrome) of known weight and then hooked up to MasterPrep. The sample was degassed at 120 °C for 12 hours. The degassed sample was weighed precisely and then transferred back to the analyzer. The temperatures for adsorption measurements was controlled by using refrigerated bath of liquid nitrogen (77 K) or liquid argon (87 K), and temperature controlled water bath (273 K and 298 K). Adsorption measurements were performed on an Autosorb-1 C (Quantachrome) volumetric analyzer using adsorbates of UHP grade.

Figure S7: Experimental Ar adsorption isotherms for , BILP-11 (orange circles), BILP-12 (blue circles) and BILP-13 (red circles) measured at 87 K. The calculated NLDFT isotherm is overlaid as open circle. Note that a fitting error of < 1 % indicates the validity of using this method for assessing the porosity of BILPs. The fitting error is indicated.

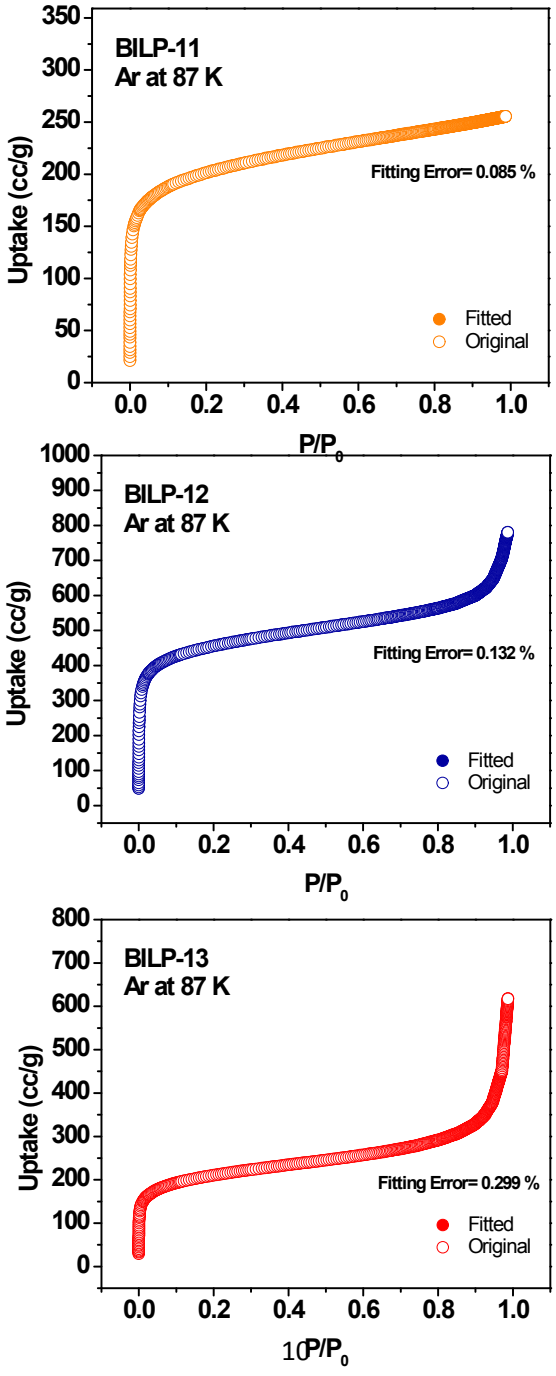

Figure S8: Pore Size Distribution of BILP-11, BILP-12, BILP-13.

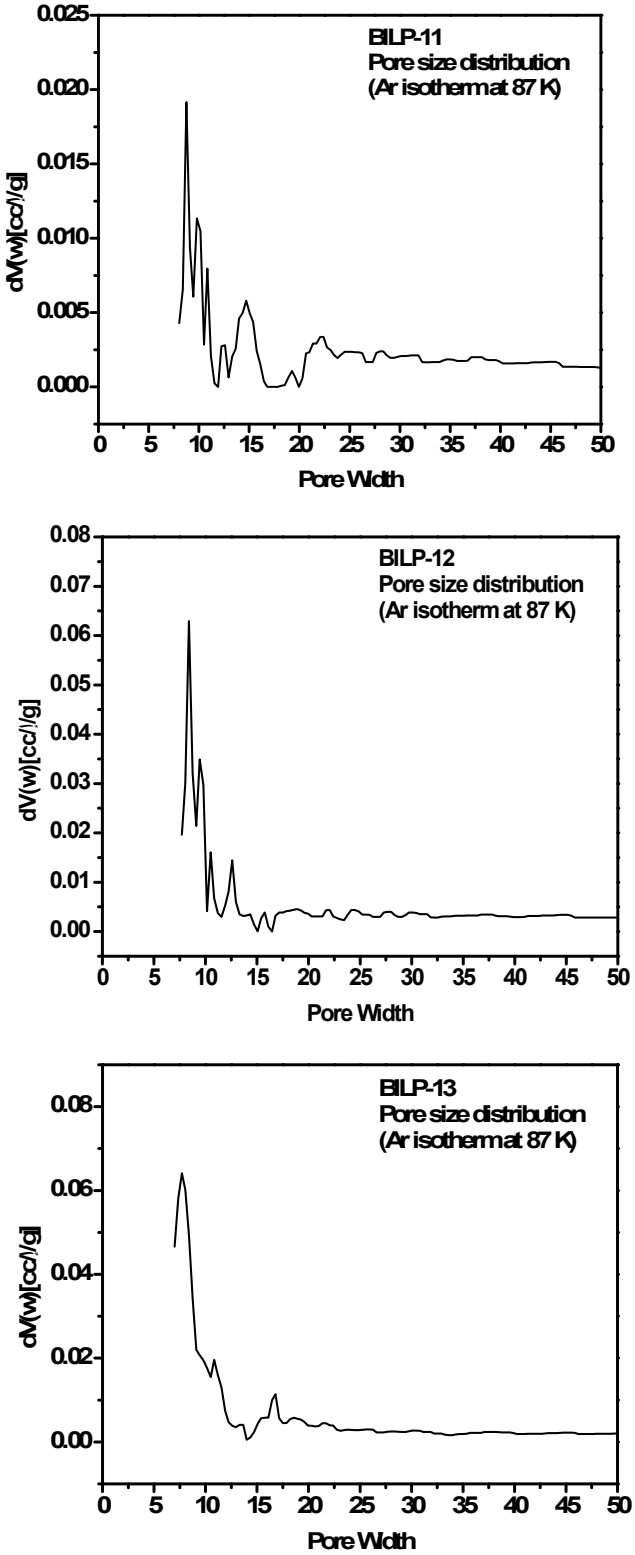

Figure S 9. Plot of the term $V(1- P/P_0)$ vs. P/P_0 for BILP-11. Only the range below $P/P_0 = 0.10$ satisfies the first consistency criterion for applying the BET theory. Inset: Plot of the linear region for the BET equation.

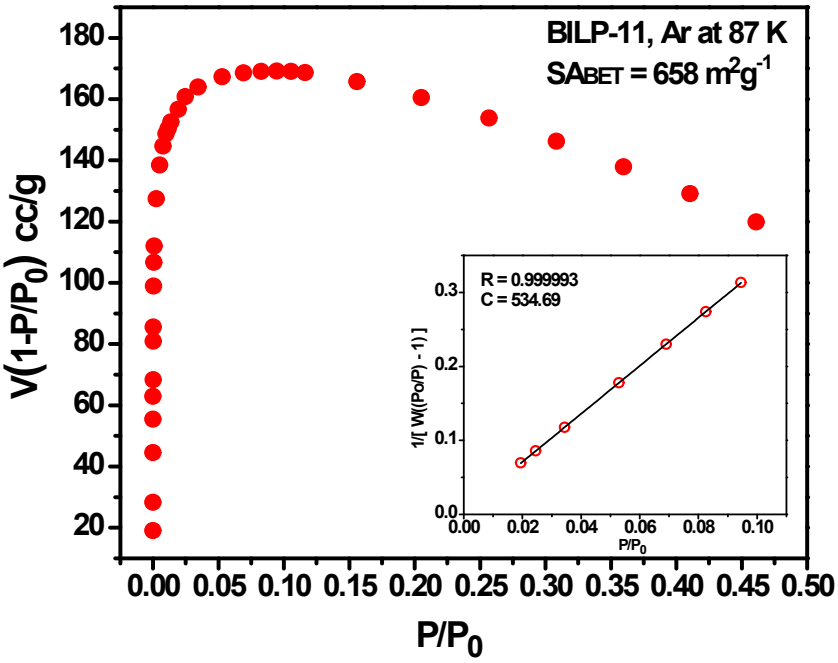

Figure S 10. Plot of the term $V(1- P/P_0)$ vs. P/P_0 for BILP-12. Only the range below $P/P_0 = 0.09$ satisfies the first consistency criterion for applying the BET theory. Inset: Plot of the linear region for the BET equation.

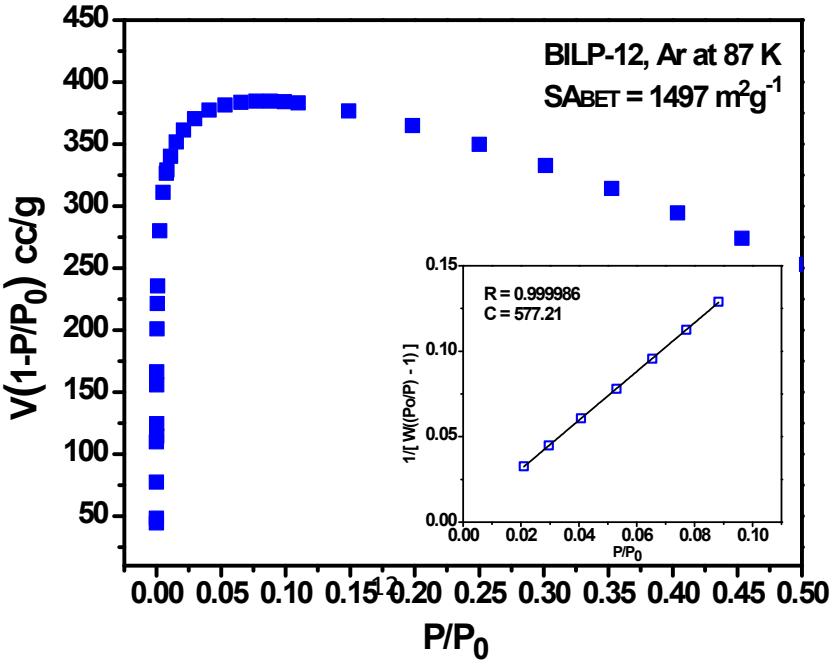

Figure S 11. Plot of the term $V(1- P/P_0)$ vs. P/P_0 for BILP-13. Only the range below $P/P_0 = 0.11$ satisfies the first consistency criterion for applying the BET theory. Inset: Plot of the linear region for the BET equation.

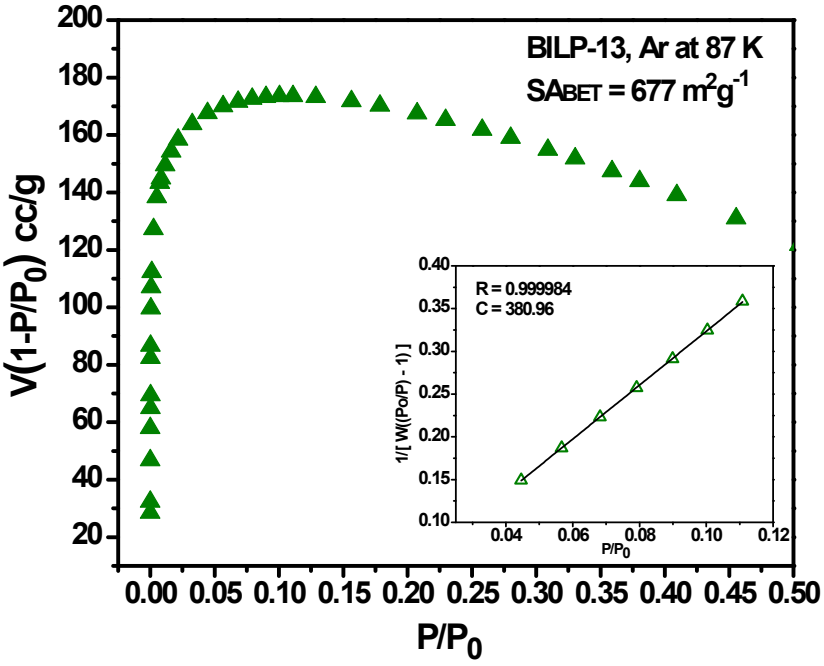

Figure S12: Gas uptake isotherms for BILP-11 (orange circles), BILP-12 (blue pentagons) and BILP-13 (red triangle) at 273 and 298 K.

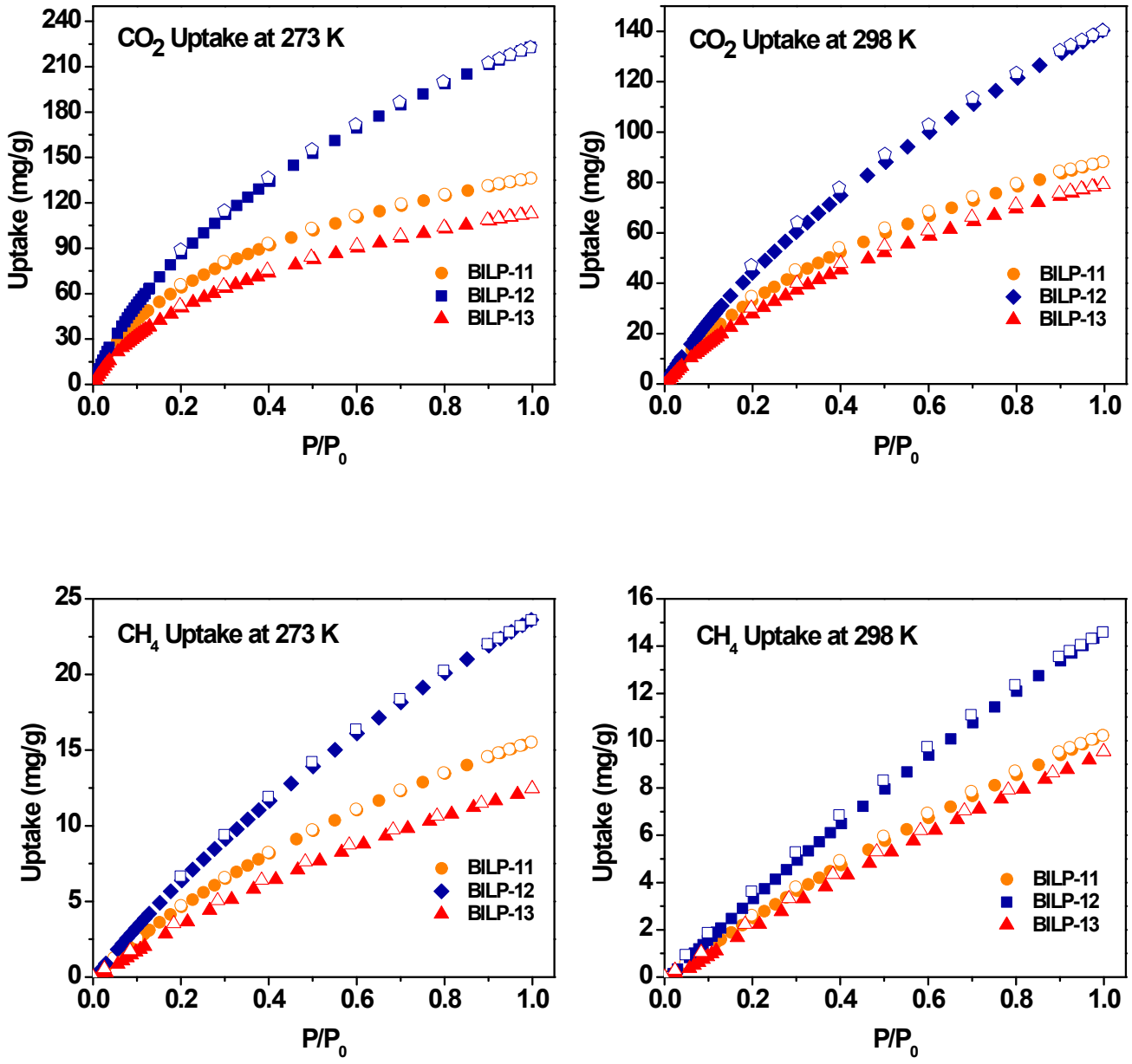

Section 3: Calculation of Isosteric heats of adsorption for BILPs

We have fitted the pure gas isotherms collected at 237 and 298 K with both viral-type and Langmuir-Freundlich equation. In both cases Clausius-Clapeyron equation employed in order to calculate isosteric heat of adsorptions of BILPs.

$$Q_{st} = RT^2\left(\frac{\partial \ln p}{\partial T}\right)_n$$

where T is the temperature, R is the universal gas constant and p is the pressure for given quantity of gas adsorbed (n). Pressure for a given n calculated from fitted isotherms.

The virial equation can be written in the form of

$$\ln p = \ln n + \frac{1}{T}\sum_{i=0}^{M} a_i n^i + \sum_{i=0}^{N} b_i n^i$$

where n is the amount adsorbed in mmol g^{-1}, p is the pressure in Torr, T is the temperature, a_i and b_i are temperature independent empirical parameters, and M and N determine the number of terms required to adequately describe the isotherm.

By applying Clausius-Clapeyron equation to virial equation, Q_{st} can be calculated according to following equation as a function of loading:

$$Q_{st} = -R\sum_{i=0}^{M} a_i n^i$$

where R is the universal gas constant (8.314 J K^{-1} mol^{-1}).

Zero-coverage (loading independent) isosteric heats of adsorption is given by

$$Q_{st} = -Ra_0$$

Langmuir-Freundlich isotherm model was also used to describe single component gas uptakes measured at 273 and 298 K. Fitting parameters obtained were then used to calculate the pressures required for the same loadings (n) at 273 and 298 K, then Clausius-Clapeyron equation were applied in order to calculate isosteric heats of adsorption.[4] Langmuir-Freundlich equation and fitting parameters are given in the next section.

Figure S13. Experimental data (symbol) and corresponding fittings (solid line) of CO_2 adsorption isotherms in BILP-11 at 273 and 298 K. Fitted curves are obtained by the virial-type expansion.

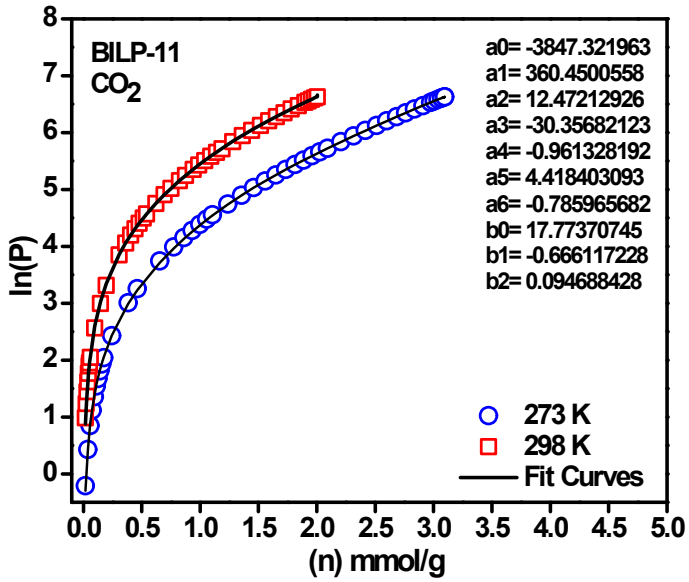

Figure S14. Experimental data (symbol) and corresponding fittings (solid line) of CO_2 adsorption isotherms in BILP-12 at 273 and 298 K. Fitted curves are obtained by the virial-type expansion.

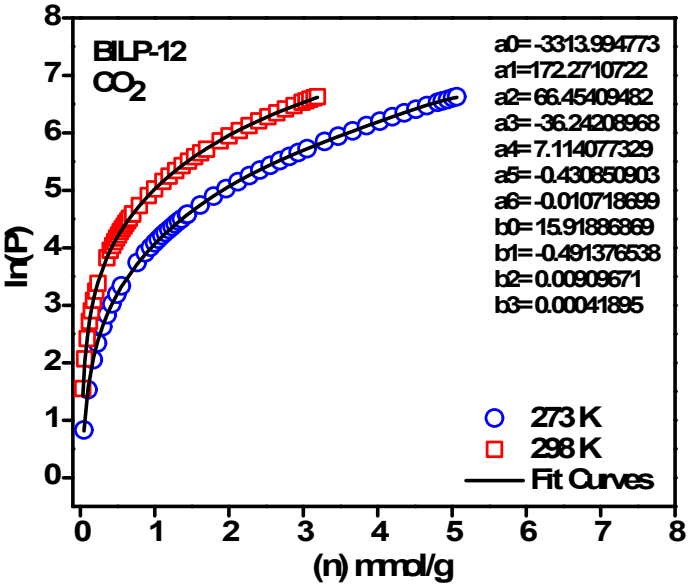

Figure S15. Experimental data (symbol) and corresponding fittings (solid line) of CO_2 adsorption isotherms in BILP-13 at 273 and 298 K. Fitted curves are obtained by the virial-type expansion.

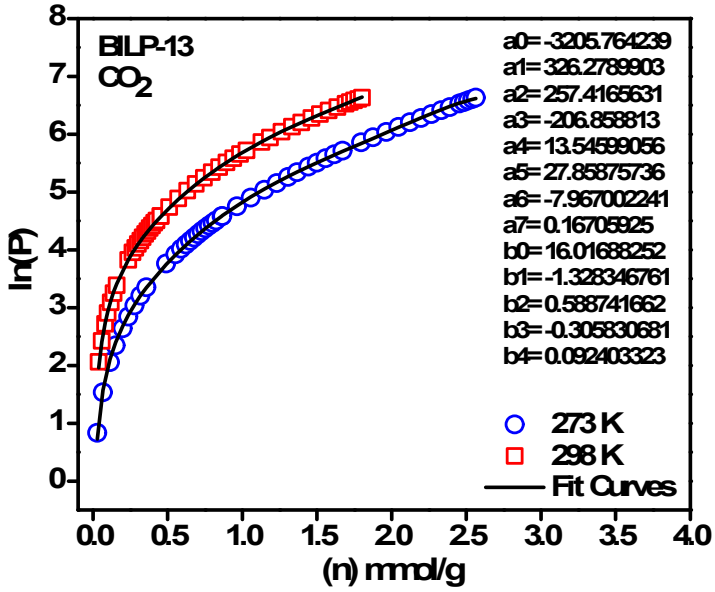

Figure S16. Experimental data (symbol) and corresponding fittings (solid line) of CH_4 adsorption isotherms in BILP-11 at 273 and 298 K. Fitted curves are obtained by the virial-type expansion.

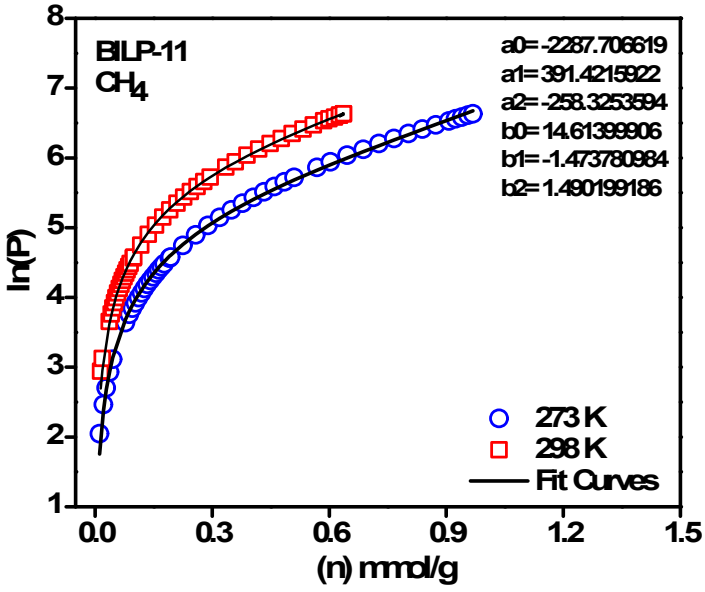

Figure S17. Experimental data (symbol) and corresponding fittings (solid line) of CH_4 adsorption isotherms in BILP-12 at 273 and 298 K. Fitted curves are obtained by the virial-type expansion.

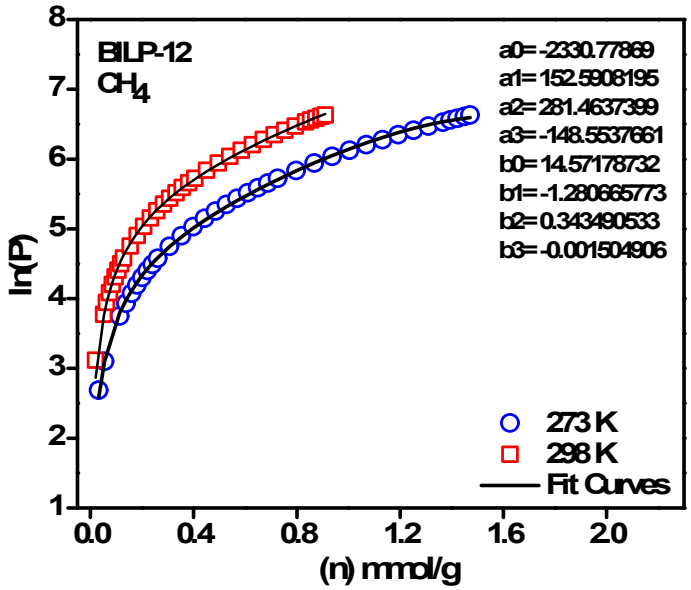

Figure S18. Experimental data (symbol) and corresponding fittings (solid line) of CH_4 adsorption isotherms in BILP-13 at 273 and 298 K. Fitted curves are obtained by the virial-type expansion.

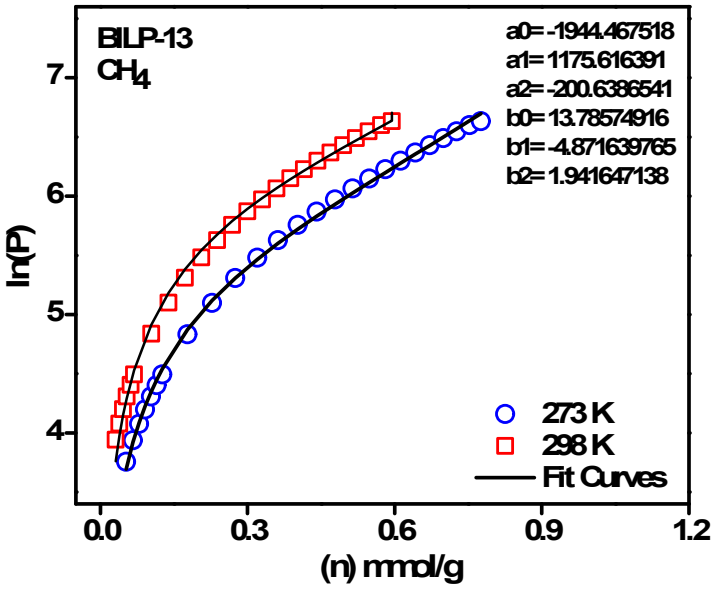

Figure S19. Isosteric heats of adsorption of methane in BILP-11, BILP-12, and BILP-13 calculated using viral-type isotherm fitting.

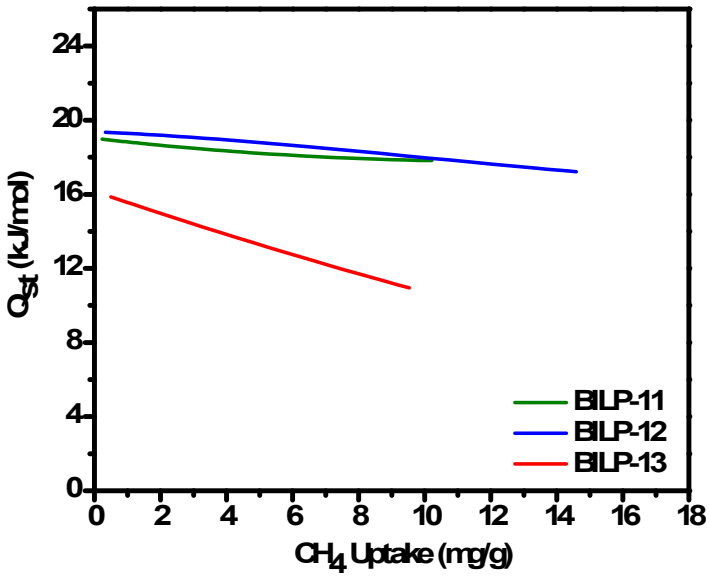

Figure S20. Isosteric heats of adsorptionof methane in BILP-11, BILP-12, and BILP-13 calculated Langmuir-Freundlich isotherm fitting.

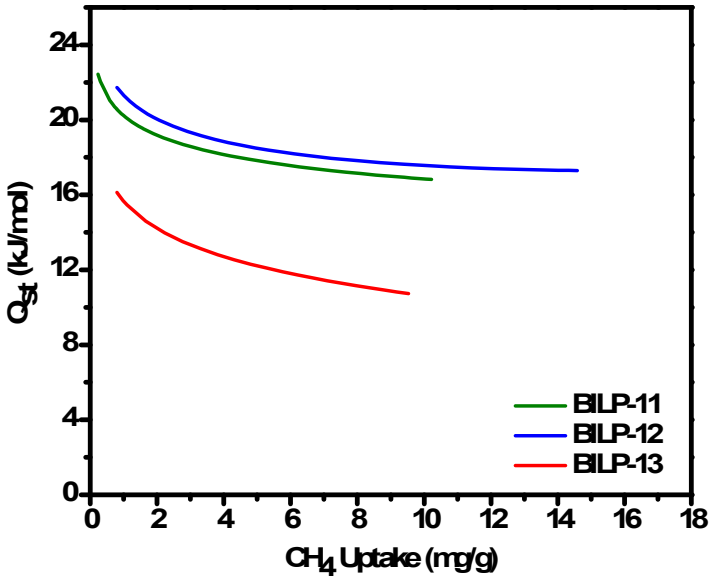

Section 4: Isotherm fittings, selectivity studies and adsorbent evaluation criteria.

The pure component isotherms of CO_2 measured at 273 and 298 K were fitted with the dual-site Langmuir-Freundlich (DSLF) model

$$q = q_A + q_B = q_{sat,A}\frac{b_A p^{\alpha_A}}{1 + b_A p^{\alpha_A}} + q_{sat,B}\frac{b_B p^{\alpha_B}}{1 + b_B p^{\alpha_B}}$$

where, q is molar loading of adsorbate (mmol g^{-1}), q_{sat} is saturation capacity (mmol g^{-1}) , b is Langmuir-Freundlich parameter ($bar^{-\alpha}$), p is bulk gas phase pressure (bar), α is the Langmuir–Freundlich exponent (dimensionless) subscripts A and B refers to site A and site B, respectively.

Since the pure component isotherms of CH_4 and N_2 do not show any inflection characteristic they were fitted with the single-site Langmuir-Freundlich (SSLF) model.

$$q = q_{sat,A}\frac{b_A p^{\alpha_A}}{1 + b_A p^{\alpha_A}}$$

Pure-component isotherm fitting parameters were then used for calculating Ideal Adsorbed Solution Theory (IAST) binary-gas adsorption selectivities, S_{ads}, defined as

$$S_{ads} = \frac{x_1/x_2}{p_1/p_2}$$

where x_i is the mole fraction of component i in the adsorbed phase and p_i is the mole fraction of component i in the bulk. [5]

x_i values were then used for calculating total amount adsorbed under mixture conditions according to following equation

$$\frac{1}{n_t} = \sum_{i=1}^{N}\left[\frac{x_i}{n_i^0}\right]$$

where n_t is the total number of adsorbed moles of gas per unit mass of adsorbent and n_i^0 is the number of moles of component i in the adsorbed phase per unit mass of adsorbent at temperature T in the absence of competing component.[5]

The adsorption amount for the component i (n_i^{ads}) in the binary mixture adsorption is calculated employing the following equation:

$$n_i^{ads} = n_t x_i$$

Using the sorbent evaluation criteria one can easily evaluate the material for possible pressure swing adsorption (PSA) and vacuum swing adsorption (VSA) applications. Recent cases have been used in literature are the following,[6 7]

1. Natural gas purification using PSA (CO_2/CH_4 : 10/90, p^{ads} = 5 bar, p^{des} = 1 bar)
2. Landfill gas separation using PSA (CO_2/CH_4 : 50/50, p^{ads} = 5 bar, p^{des} = 1 bar)
3. Landfill gas separation using VSA (CO_2/CH_4 : 50/50, p^{ads} = 1 bar, p^{des} = 0.1 bar)
4. Flue gas separation using VSA (CO_2/N_2 : 10/90, p^{ads} = 1 bar, p^{des} = 0.1 bar)

Figure S21: CO_2 , CH_4 and N_2 uptakes of BILP-11, BILP-12 and BILP-13 at 273 K and 298 K.

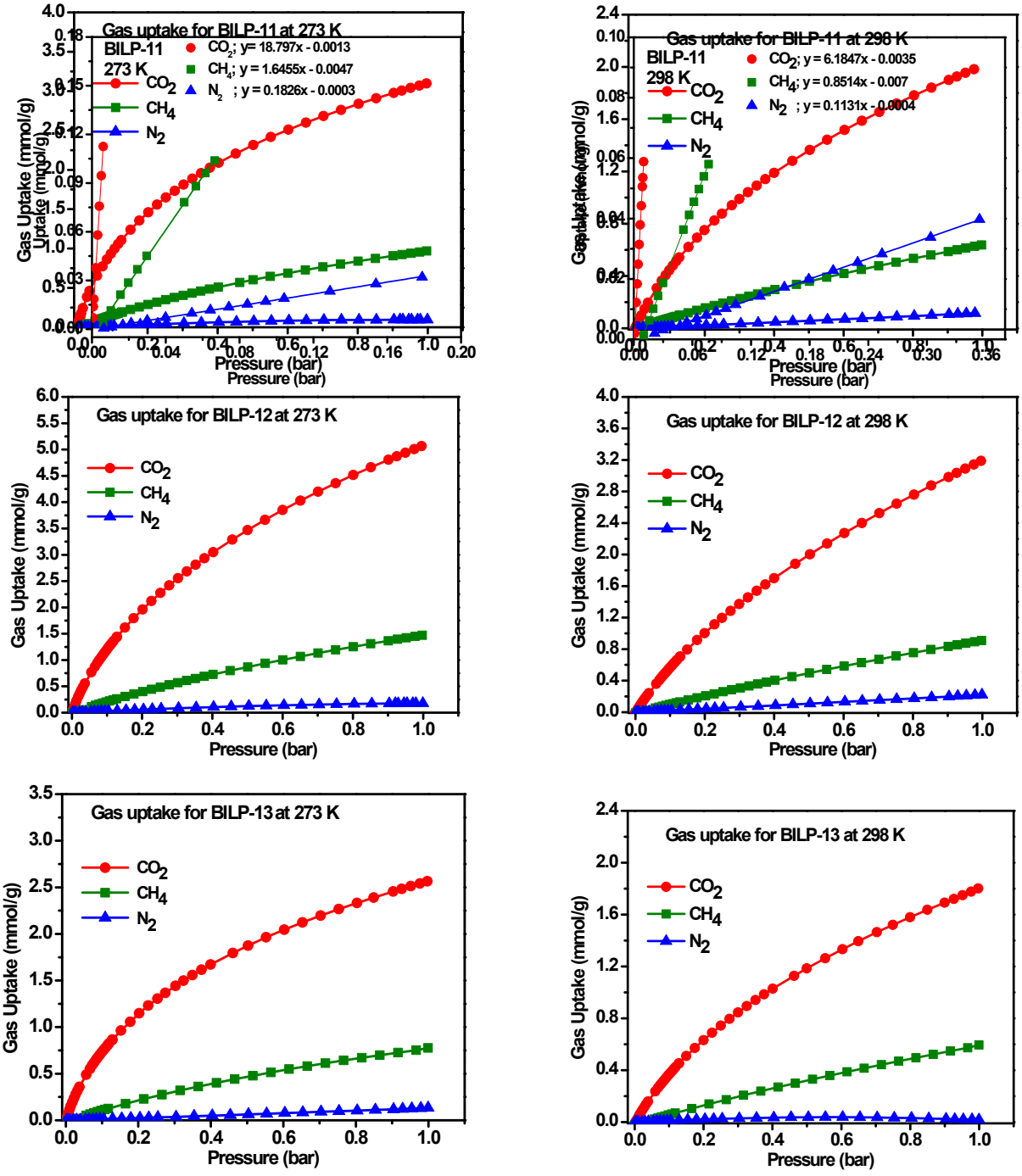

Figure S22: Gas uptake selectivity studies for BILP-11, BILP-12 and BILP-13 at 273 and 298 K (CO_2 over CH_4 and N_2).

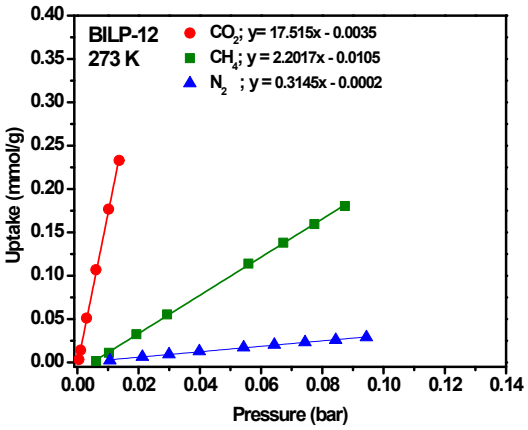
BILP-12
273 K
CO2; y= 17.515x - 0.0035
CH4; y = 2.2017x - 0.0105
N2 ; y = 0.3145x - 0.0002
Uptake (mmol/g)
Pressure (bar)

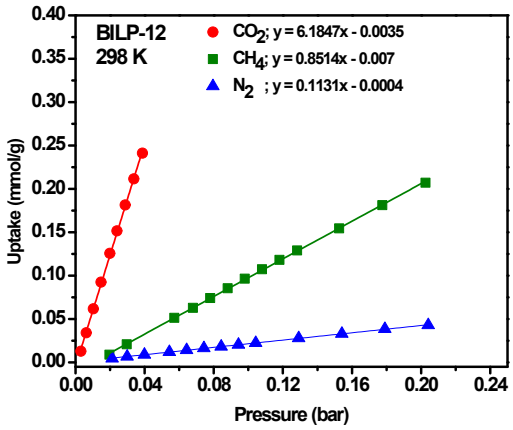
BILP-12
298 K
CO2; y = 6.1847x - 0.0035
CH4; y = 0.8514x - 0.007
N2 ; y = 0.1131x - 0.0004
Uptake (mmol/g)
Pressure (bar)

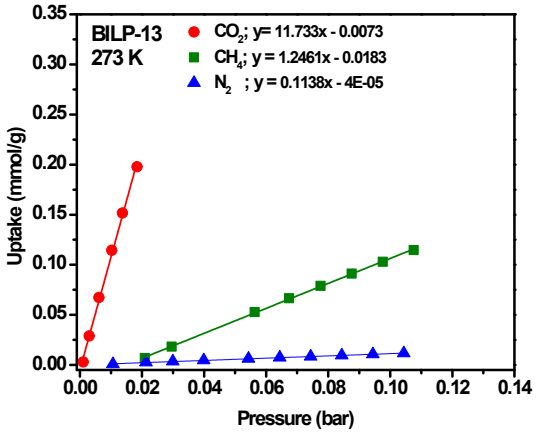
BILP-13
273 K
CO2; y= 11.733x - 0.0073
CH4; y = 1.2461x - 0.0183
N2 ; y = 0.1138x - 4E-05
Uptake (mmol/g)
Pressure (bar)

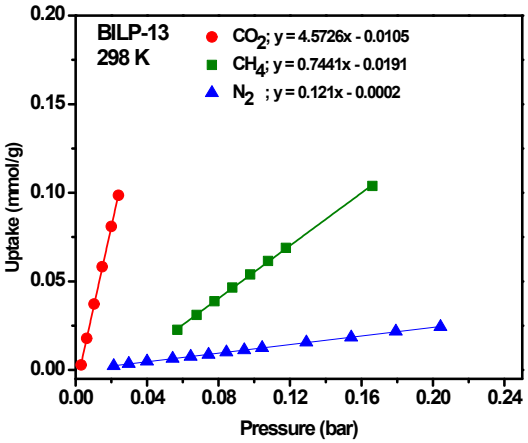
BILP-13
298 K
CO2; y = 4.5726x - 0.0105
CH4; y = 0.7441x - 0.0191
N2 ; y = 0.121x - 0.0002
Uptake (mmol/g)
Pressure (bar)

Table S2. Langmuir-Freundlich fitting parameters of CO_2, CH_4, and N_2 adsorption isotherms in BILP-11 at 298 K and low pressures (0-1 bar).

	$q_{sat,A}$ *(mmol/g)*	b_A *($bar^{-\alpha}$)*	α_A *dimensionless*	$q_{sat,B}$ *(mmol/g)*	b_B *($bar^{-\alpha}$)*	α_B *dimensionless*	*Reduced* χ^2	*Adj.* R^2
CO_2	4.63186	0.38932	0.99595	0.86275	4.58749	0.98666	1.86E-06	1
CH_4	2.39111	0.36226	1.03824				2.14E-06	0.99995
N_2	7.00487	0.01702	1.04926				1.67E-07	0.9999

Figure S23. Experimental data and corresponding fittings of CO_2, CH_4, and N_2 adsorption isotherms in BILP-11 at 298 K and low pressures (0-1 bar).

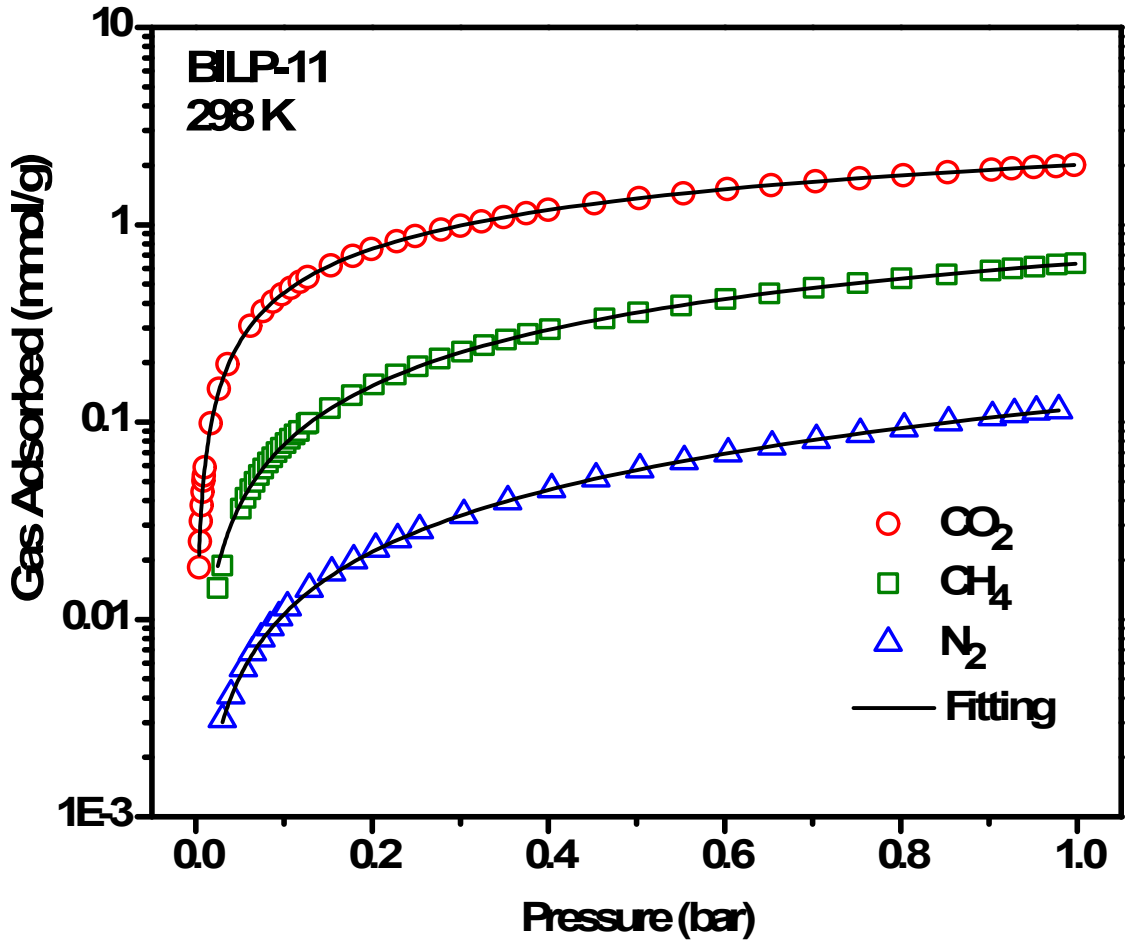

Table S3. Langmuir-Freundlich fitting parameters of CO_2, CH_4, and N_2 adsorption isotherms in BILP-12 at 298 K low pressures (0-1 bar).

	$q_{sat,A}$ *(mmol/g)*	b_A *($bar^{-\alpha}$)*	α_A *dimensionless*	$q_{sat,B}$ *(mmol/g)*	b_B *($bar^{-\alpha}$)*	α_B *dimensionless*	*Reduced* χ^2	*Adj.* R^2
CO_2	11.53246	0.24064	1.03760	1.22272	3.59695	1.01274	1.86E-06	1
CH_4	3.84089	0.30965	1.06675				2.14E-06	0.99995
N_2	12.48505	0.01789	1.03264				1.67E-07	0.9999

Figure S24. Experimental data and corresponding fittings of CO_2, CH_4, and N_2 adsorption isotherms in BILP-12 at 298 K and low pressures (0-1 bar).

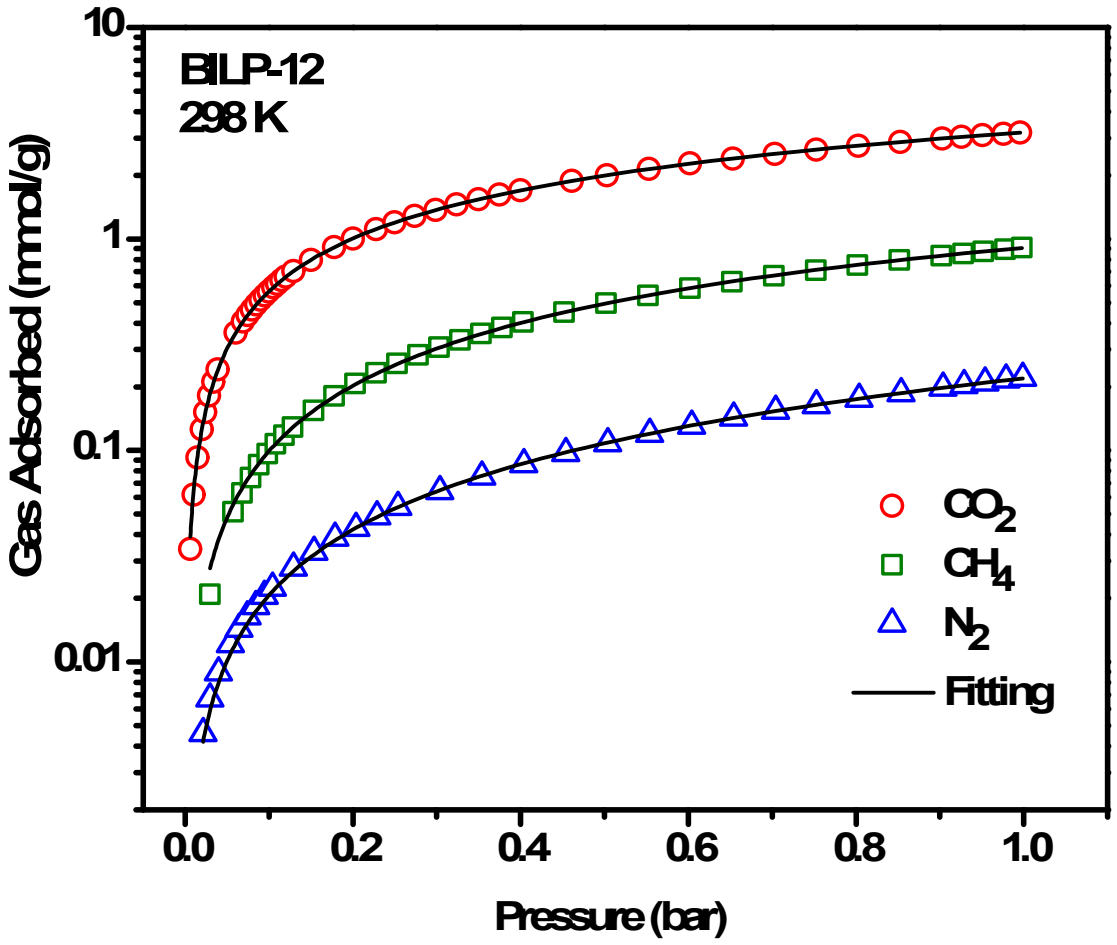

Table S4. Langmuir-Freundlich fitting parameters of CO_2, CH_4, and N_2 adsorption isotherms in BILP-13 at 298 K low pressures (0-1 bar).

	$q_{sat,A}$ *(mmol/g)*	b_A *($bar^{-\alpha}$)*	α_A *dimensionless*	$q_{sat,B}$ *(mmol/g)*	b_B *($bar^{-\alpha}$)*	α_B *dimensionless*	*Reduced* χ^2	*Adj.* R^2
CO_2	4.31374	0.41225	1.05511	0.62258	6.56056	1.09024	3.22E-06	0.99999
CH_4	1.73943	0.50917	1.17534				1.29E-05	0.99966
N_2	15.47574	0.00859	1.06806				3.55E-07	0.99984

Figure S25. Experimental data and corresponding fittings of CO_2, CH_4, and N_2 adsorption isotherms in BILP-13 at 298 K and low pressures (0-1 bar).

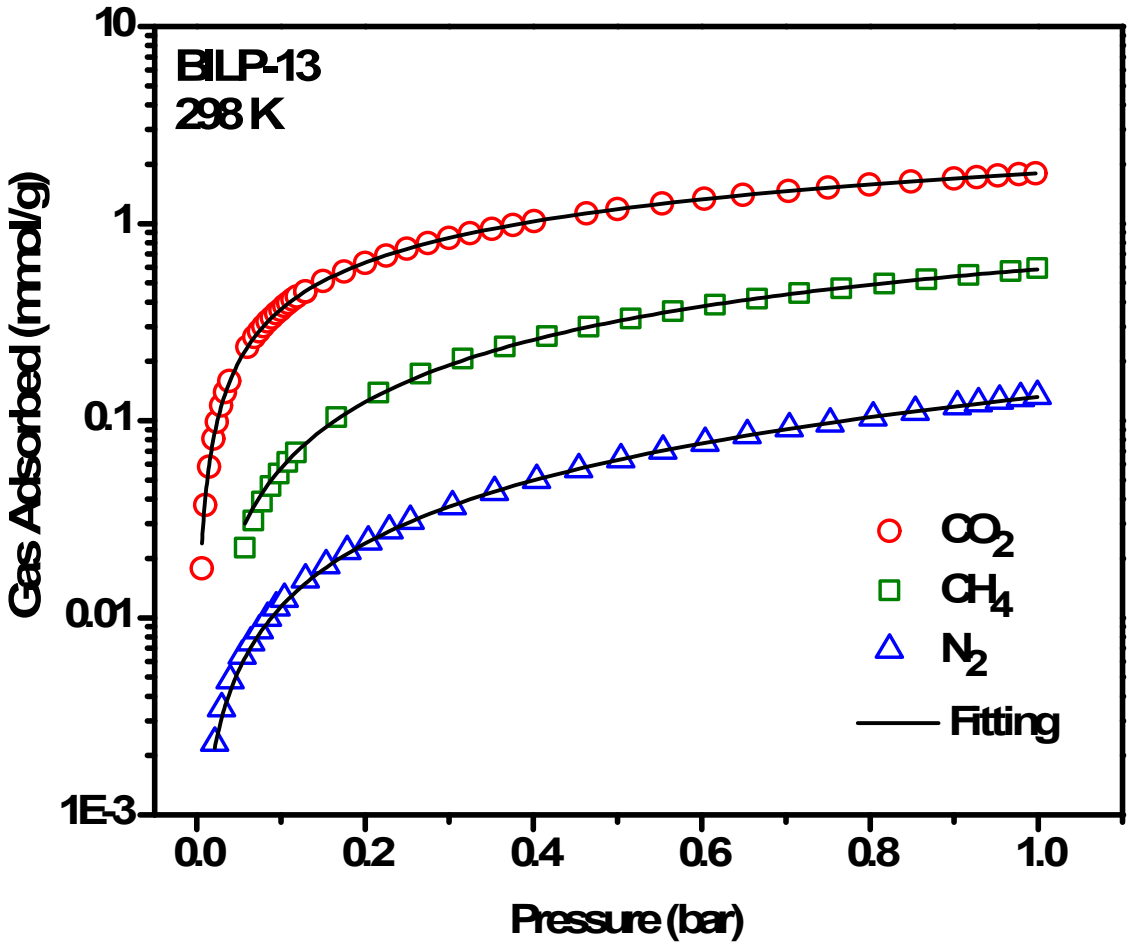

Table S5. Langmuir-Freundlich fitting parameters of CO_2 adsorption isotherms in BILP-11, BILP-12 and BILP-13 at 273 K and low pressures (0-1 bar).

	$q_{sat,A}$ *(mmol/g)*	b_A *($bar^{-\alpha}$)*	α_A *dimensionless*	$q_{sat,B}$ *(mmol/g)*	b_B *($bar^{-\alpha}$)*	α_B *dimensionless*	*Reduced* χ^2	*Adj.* R^2
BILP-11	2.55473	3.92609	0.87342	2.55473	0.71021	1.31074	9.58E-06	0.99999
BILP-12	11.71108	0.47642	0.93745	1.52437	5.59862	0.94541	7.01E-06	1
BILP-13	2.15718	3.79148	0.91630	2.15718	0.65884	1.40823	8.59E-06	0.99999

Figure S26. Experimental data and corresponding fittings of CO_2 adsorption isotherms in BILP-11, BILP-12 and BILP-13 at 273 K and low pressures (0-1 bar).

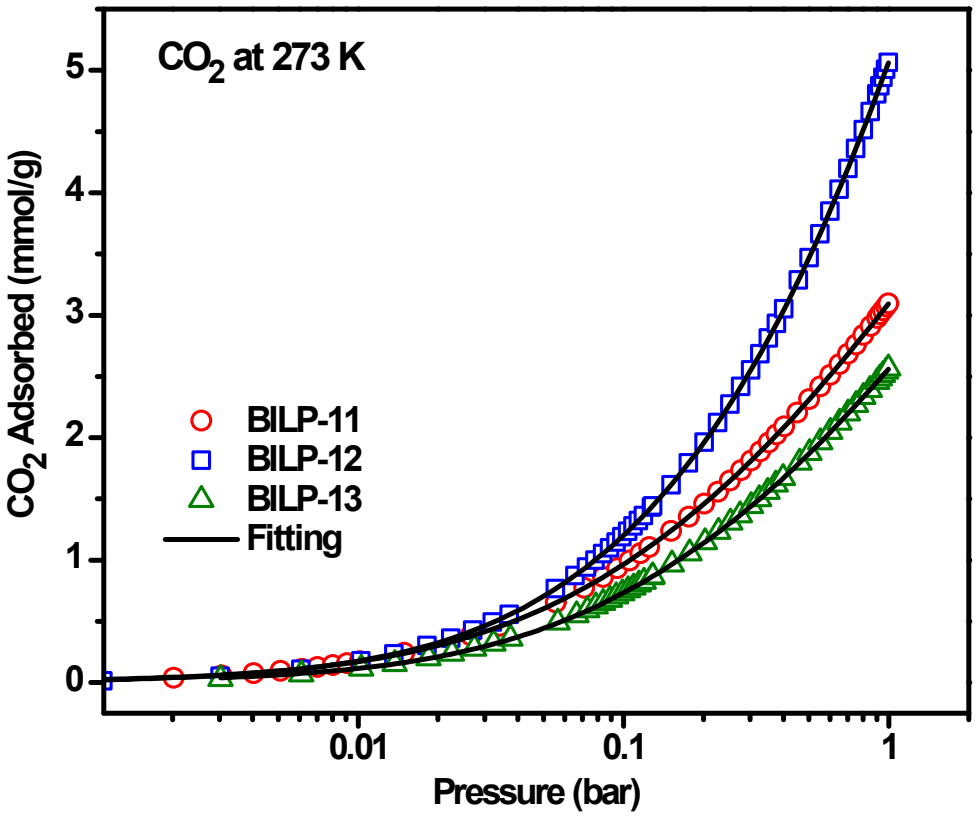

Table S6. Langmuir-Freundlich fitting parameters of CH_4 adsorption isotherms in BILP-11, BILP-12 and BILP-13 at 273 K and low pressures (0-1 bar).

	$q_{sat,A}$ *(mmol/g)*	b_A *($bar^{-\alpha}$)*	α_A *dimensionless*	*Reduced* χ^2	*Adj.* R^2
BILP-11	2.53960	0.61492	0.98134	5.01E-06	0.99995
BILP-12	4.87729	0.43123	0.99132	1.67E-05	0.99993
BILP-13	1.81128	0.73637	1.07923	2.21E-05	0.99967

Figure S27. Experimental data and corresponding fittings of CH_4 adsorption isotherms in BILP-11, BILP-12 and BILP-13 at 273 K and low pressures (0-1 bar).

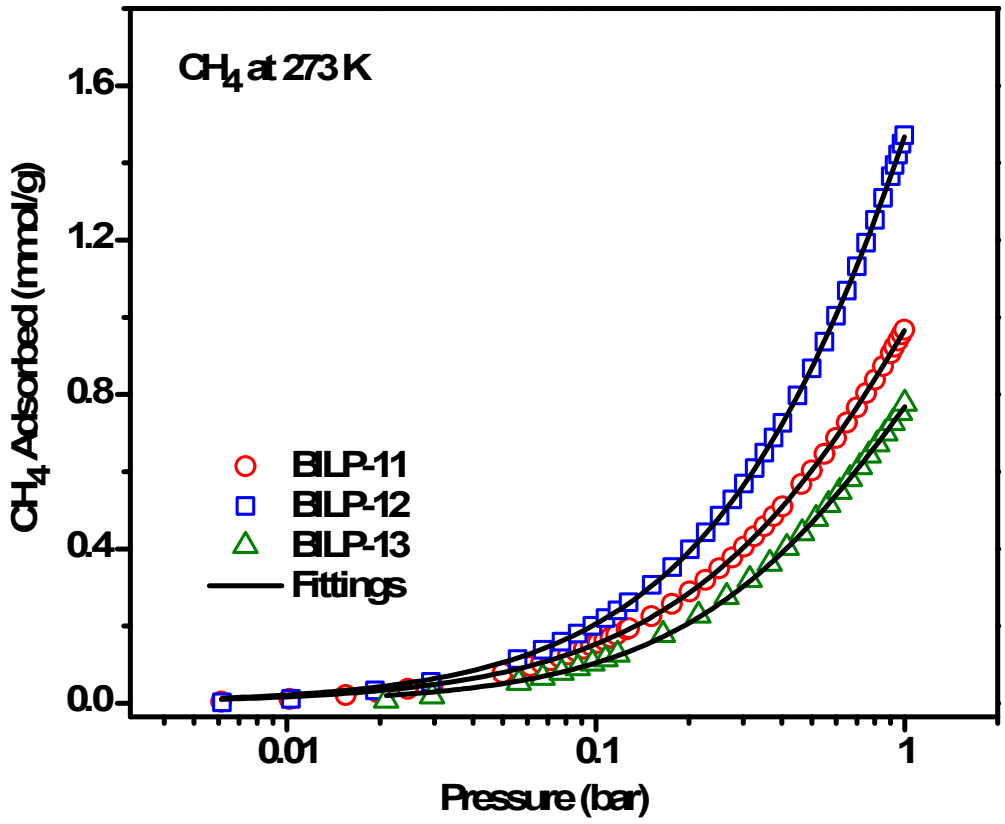

Section 5: High-Pressure (1-10 bar) Gas Adsorption Measurements and Their Corresponding Isotherm Fittings

High pressure sorption isotherms were run using a VTI HPVA-100 volumetric analyzer. Ultrahigh purity helium (99.999%) was used to calibrate the free volume in the sample cell before each measurement. High pressure data was collected using ultrahigh purity H_2 (99.999%), CO_2 (99.99%) and CH_4 (99.999%) obtained from Airgas Inc. (Radnor, PA). Free space measurements were performed prior to data collection utilizing ultra-high purity helium to establish the appropriate cold zone compensation factors. Absolute gas uptakes were calculated according to literature methods using NIST Thermochemical Properties of Fluid Systems.[8, 9]

Table S7. Langmuir-Freundlich fitting parameters of CO_2 and CH_4 total adsorption isotherms in BILP-11 at 298 K and high pressures (1-10 bar).

	$q_{sat,A}$ *(mmol/g)*	b_A *($bar^{-\alpha}$)*	α_A *dimensionless*	$q_{sat,B}$ *(mmol/g)*	b_B *($bar^{-\alpha}$)*	α_B *dimensionless*	*Reduced* χ^2	*Adj.* R^2
CO_2	8.78923	0.23720	0.58989	1.13471	0.00027	3.48432	1.02E-04	0.99985
CH_4	82.17967	0.00611	0.63652				9.22E-05	0.99955

Figure S28. Experimental data and corresponding fittings of CO_2 and CH_4 total adsorption isotherms in BILP-11 at 298 K and high pressures (1-10 bar).

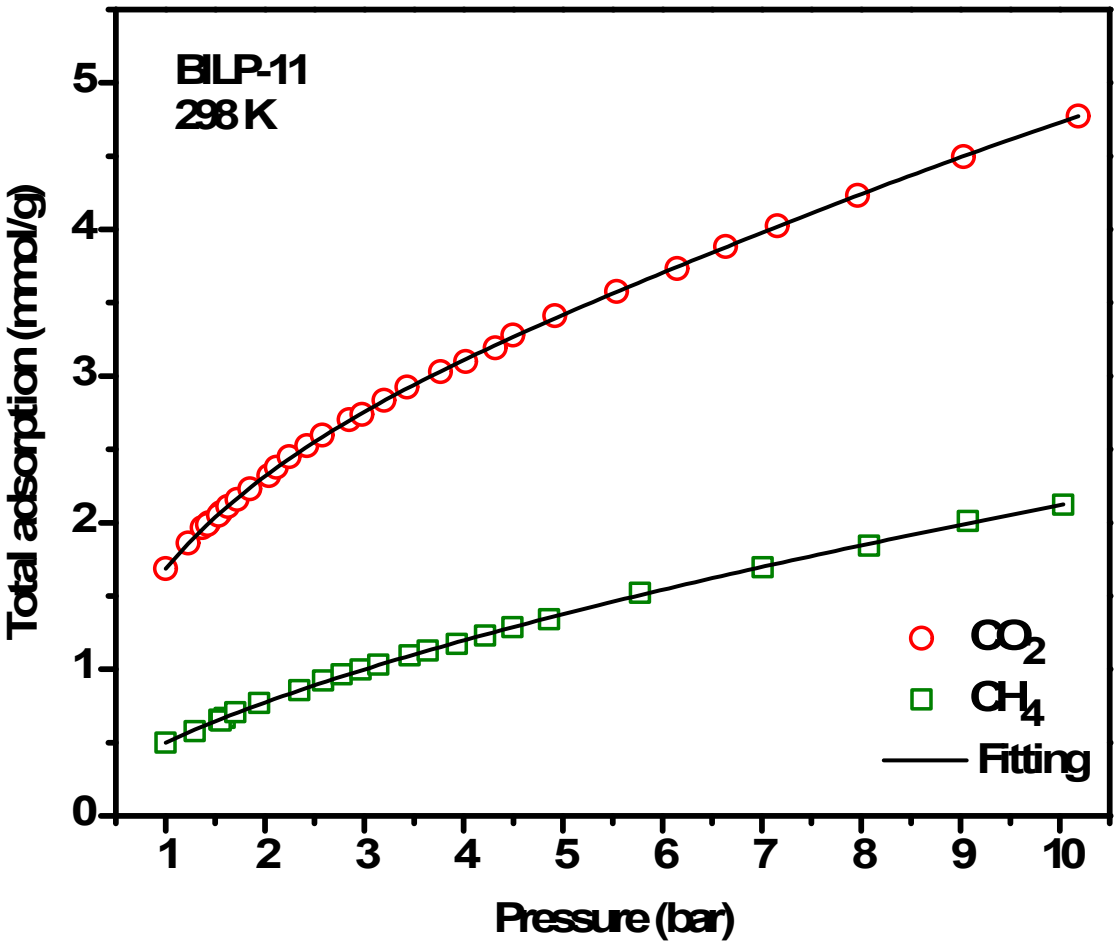

Table S8. Langmuir-Freundlich fitting parameters of CO_2 and CH_4 total adsorption isotherms in BILP-12 at 298 K and high pressures (1-10 bar).

	$q_{sat,A}$ *(mmol/g)*	b_A *($bar^{-\alpha}$)*	α_A *dimensionless*	$q_{sat,B}$ *(mmol/g)*	b_B *($bar^{-\alpha}$)*	α_B *dimensionless*	*Reduced* χ^2	*Adj.* R^2
CO_2	0.11207	0.10000	25.96054	21.42649	0.16300	0.68351	5.84E-04	0.99982
CH_4	12.02378	0.08736	0.80664				6.83E-05	0.99993

Figure S29. Experimental data and corresponding fittings of CO_2 and CH_4 total adsorption isotherms in BILP-12 at 298 K and high pressures (1-10 bar).

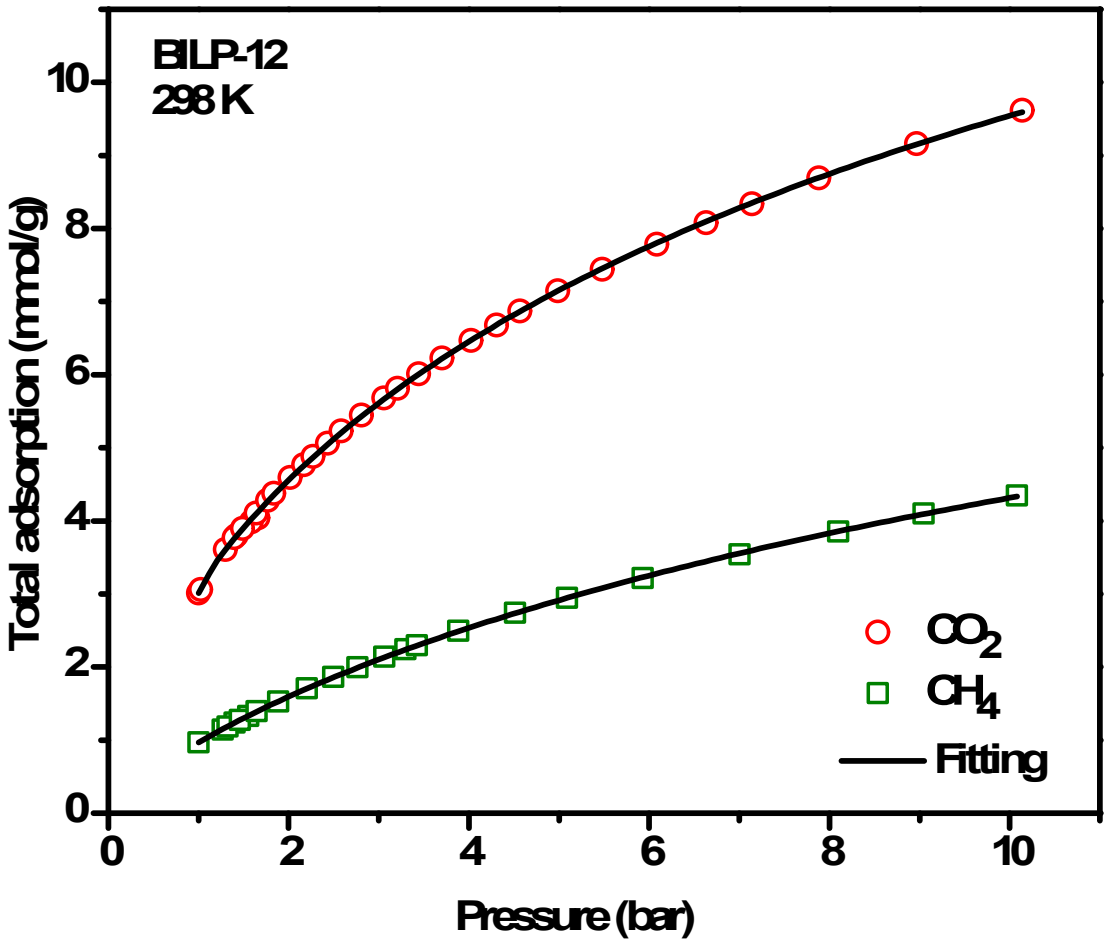

Table S9. Langmuir-Freundlich fitting parameters of CO_2 and CH_4 total adsorption isotherms in BILP-13 at 298 K and high pressures (1-10 bar).

	$q_{sat,A}$ *(mmol/g)*	b_A *($bar^{-\alpha}$)*	α_A *dimensionless*	$q_{sat,B}$ *(mmol/g)*	b_B *($bar^{-\alpha}$)*	α_B *dimensionless*	*Reduced* χ^2	*Adj.* R^2
CO_2	4.93109	0.00418	1.87579	4.93109	0.50425	0.80475	9.13E-05	0.99988
CH_4	16.90487	0.03233	0.68995				3.13E-05	0.99987

Figure S30. Experimental data and corresponding fittings of CO_2 and CH_4 total adsorption isotherms in BILP-13 at 298 K and high pressures (1-10 bar).

References

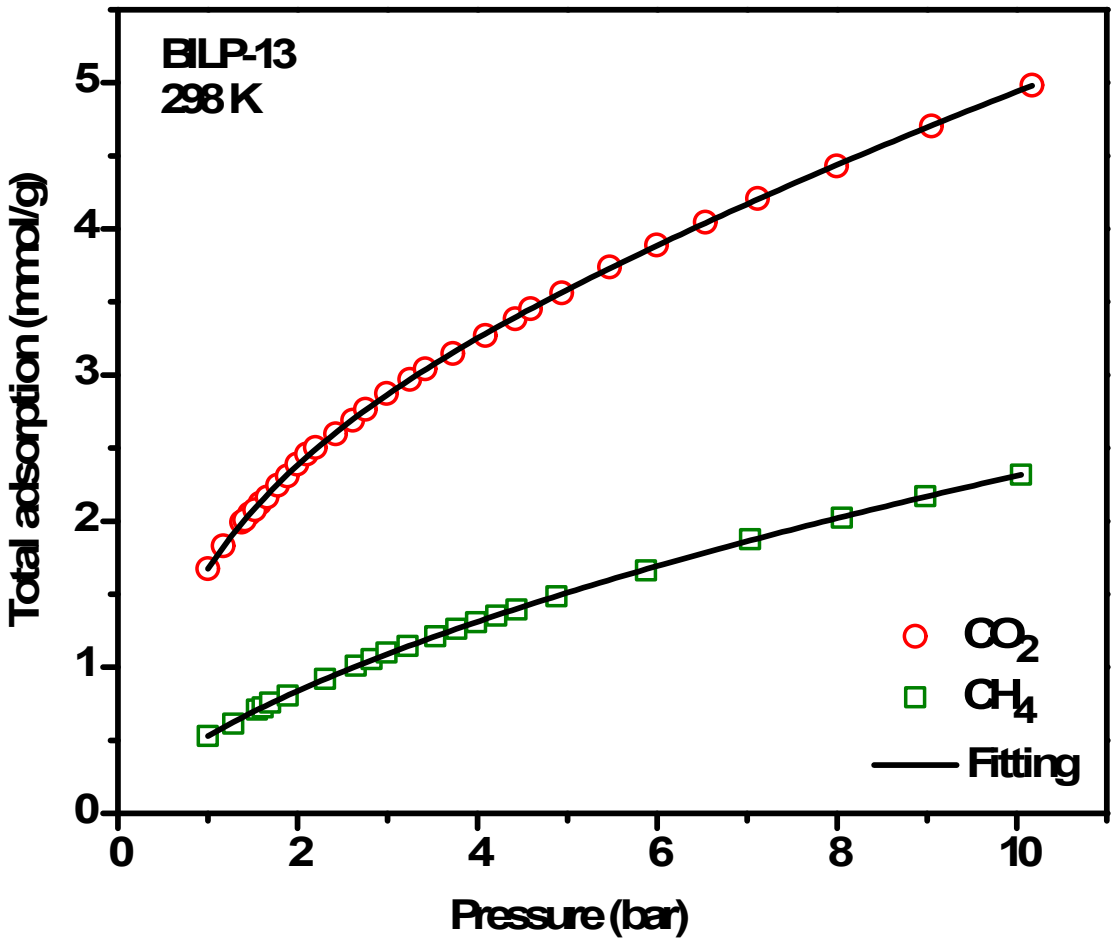

References

1. M. G. Rabbani and H. M. El-Kaderi, *Chem. Mater.*, 2012, 24, 1511-1517.

2. M. G. Rabbani, T. E. Reich, R. M. Kassab, K. T. Jackson and H. M. El-Kaderi, *Chem. Commun.*, 2012, 48, 1141-1143.

3. M. G. Rabbani and H. M. El-Kaderi, *Chem. Mater.*, 2011, 23, 1650-1653.

4. W. L. Queen, E. D. Bloch, C. M. Brown, M. R. Hudson, J. A. Mason, L. J. Murray, A. J. Ramirez-Cuesta, V. K. Peterson and J. R. Long, *Dalton T*, 2012, 41, 4180-4187.

5. A. L. Myers and J. M. Prausnitz, *Aiche. J.*, 1965, 11, 121-127.

6. C. E. Wilmer, O. K. Farha, Y. S. Bae, J. T. Hupp and R. Q. Snurr, *Energ. Environ. Sci.*, 2012, 5, 9849-9856.

7. Y. S. Bae and R. Q. Snurr, *Angew. Chem., Int. Edit.*, 2011, 50, 11586-11596.

8. H. Furukawa, M. A. Miller and O. M. Yaghi, *J. Mater. Chem.*, 2007, 17, 3197-3204.

9. N. C. W. T. P. o. F. S. http://webbook.nist.gov/chemistry/fluid/.